Nano TiO$_2$–Au–KI film sensor for the electrocatalytic oxidation of hydrogen peroxide

Soundappan Thiagarajan, Buo-Wei Su, Shen-Ming Chen*

Electro analysis and Bioelectrochemistry Laboratory, Department of Chemical Engineering and Biotechnology, National Taipei University of Technology, No.1, Section 3, Chung-Hsiao East Road, Taipei 106, Taiwan, ROC

ARTICLE INFO

ABSTRACT

A glassy carbon and indium tin oxide (ITO) electrodes have been modified with the nano TiO$_2$–Au–KI film by the adsorption of TiO$_2$ nanoparticles on the electrodes followed with the electrochemical depositions of nano Au and KI film. Further the nano TiO$_2$–Au–KI film modified ITO was examined by scanning electron microscopy (SEM) and atomic force microscopy (AFM) techniques. From the microscopic results, the adsorbed nano TiO$_2$ particles size were found in the range of 70–100 nm. Here the electrochemical depositions of nano Au were formed as a flower shape were in the size range of 230 nm to 1 μm. Next the electrochemical behavior of nano TiO$_2$–Au–KI film has been examined in different pH solutions. The nano TiO$_2$–Au–KI film modified glassy carbon electrode (GCE) showed good electrocatalytic activity towards the oxidation of H$_2$O$_2$ in phosphate buffer solutions (pH 7.0). The linear range of detection for H$_2$O$_2$ oxidation using nano TiO$_2$–Au–KI film was found as 1×10^{-5} to 1×10^{-4} M and 1×10^{-9} to 1×10^{-7} M in CV and differential pulse voltammetry (DPV) techniques. The practical applications of nano TiO$_2$–Au–KI film was evaluated by analyzing the real samples such as antiseptic and contact lens cleaner solutions containing H$_2$O$_2$.

© 2008 Elsevier B.V. All rights reserved.

1. Introduction

Hydrogen peroxide has been used as antiseptic and antibacterial agent for many years due to its oxidizing effect. It was used by hospitals, doctors, and dentists in sterilizing, cleaning, and treating everything from floors to root canal procedures. Further H$_2$O$_2$ acts as a powerful oxidizing agent, so it could be applied in so many organic compound synthesis reactions [1]. The biological systems will be directly affected by hydrogen peroxide; therefore, the central nervous system diseases could be formed [2]. According to these reasons, there is a need of a sensor to detect the H$_2$O$_2$ in clinical and environmental applications [3]. Further the detection and determination of H$_2$O$_2$ can be done in several methods like spectrophotometric [4], titrimetric [5], fluorescence [6], phosphorescence [7] and chromatographic methods [8]. Although these methods exhibit obvious result for the determination of H$_2$O$_2$, they still have their own technical drawbacks and some of them were quite expensive. Generally in electrochemical analysis, the reduction or oxidation of hydrogen peroxide is not applicable at bare electrodes. At the bare electrode, it shows the slow electrode kinetics and high over potential required for this redox reaction. To overcome this problem, the modified electrodes have been widely

applied [9]. Further the modified electrodes have shown interesting ability toward hydrogen peroxide detection. But they exhibited with many problems linked to the film deposition process, its toxicity, poor repeatability, and stability. Also the sensitivity of the modified electrodes was restricted to micro molar concentrations. For these reasons, there is a need to develop a simple and reliable methods for fabrication of novel sensor for hydrogen peroxide detection at nanomolar or in lower concentration range.

The self-assembly method is one of the experimentally simplest and cheapest one for the fabrication of nanoparticles from the solution to electrode surface. In self-assembly techniques, the electrostatic adsorption based oppositely charged materials was developed and has been a promising method for the fabrication of thin films [10]. The self-assembled nano particles have been widely used in the modification of surface properties like materials, sensors, microelectronics, and molecular devices [11]. On the other hand, the metal and metal oxide particles in the form of nano size exhibited in higher surface area to reduce the cost and very easily immobilized on electrode surfaces, having their potential applications in the relative biomedical field. Various metal oxide particles have been used for the determination of H$_2$O$_2$. For example, nickel oxide [12], iron oxide [13], zirconium oxide [14], tungsten oxide [15], manganese oxide [16], and cobalt oxide [17] have been successfully used for their applications in fabrication of hydrogen peroxide sensor. Likewise, the titanium oxide nano particles became apparent and fascinating in the electrochemistry field. It

* Corresponding author. Tel.: +886 2270 17147; fax: +886 2270 25238.
E-mail address: smchen78@ms15.hinet.net (S.-M. Chen).

has higher reactivity, good biocompatibility and can be applied in a wide range in life science and medicinal fields. Further it has been reported as an electron acceptor and transport material for the hybrid polymer/TiO$_2$ cells [18] and dye-sensitized cells [19]. In the extended view, the attractive nature of the electrode by using TiO$_2$ were in wide range of applications such as long time chemical stability, insertion host capacity and conductive properties [20]. TiO$_2$ material was also used in catalysis [21], solar energy conversion [22], electro chromic devices and in biological applications [23]. In self-assembly method, the positively charged TiO$_2$ nano particles were reported [24]. Further the self-assembled polyaniline/TiO$_2$ nanocomposite ultrathin films were applied for the photoelectrochemical applications [25].

The electrodes modified with other metals such as; ruthenium [26], silver [27], platinum [28], gold [29], and rhodium [30] have been used for micro molar detection of H$_2$O$_2$. In these methods, the gold nano particles play an important role in nano structured assemblies. Nano structured Au showed higher electro catalytic activity than the bulk Au [31,32]. At present the desired shape and size of the nanoparticles ascertained obvious changes in their catalytic activities [33,34]. For instance, the flower-shaped Au nanoparticles exhibited obvious electrocatalytic catalytic properties for the oxidation of methanol and oxygen reduction reactions [35]. In particular, the modifications of TiO$_2$ with gold nanoparticles were applied for the photo catalytic degradation reactions [36]. TiO$_2$ nano tubes with supported gold and copper particles exhibited efficient catalytic performance for CO oxidation [37]. The Au/TiO$_2$ catalysts for the selective oxidation of glucose [38], the TiO$_2$–Au nano composite film for nitric oxide oxidation [39] were reported. The TiO$_2$ nanoparticles and gold nanoparticles based amperometric immune sensor [40], potentiodynamically formed Au/TiO$_2$ composite surfaces for oxygen reduction reactions [41] have been reported.

Next in halogens, the iodine has an important role in the electrode modification process. It has the highest polarizability and binds strongly with transition metal electrodes. Further the I$^-$ adlayer modified electrodes were applied for the enhanced electrochemical oxidation [42], reduction [43,44] and the cathodic detection of H$_2$O$_2$ [45]. Thus, the modification of nanoparticles with iodide layer will show good electrocatalytic properties for H$_2$O$_2$ detection. In this study, for the first time, we are reporting the adsorption of nano TiO$_2$ with electrochemical depositions of flower shaped nano Au and KI film modified glassy carbon electrode (GCE), for the electro catalytic oxidation of H$_2$O$_2$. Further the electrochemical properties, stability, pH effect, and kinetic parameters of the proposed film were evaluated. The surface morphological analyses of the proposed film were done by using scanning electron microscopy (SEM) and atomic force microscopy (AFM) techniques. The proposed film modified GCE showed good electrocatalytic oxidation reactions of H$_2$O$_2$. Furthermore, the proposed film has been examined for the detection of H$_2$O$_2$ in real samples, respectively.

2. Experimental

2.1. Reagents

KAuCl$_4$·3H$_2$O was obtained from Strem chemicals (USA). Nano TiO$_2$ suspension was purchased from Ever light chemicals (Taiwan). KI was obtained from Wako chemicals (USA). H$_2$O$_2$ (30%) was purchased from Sigma–Aldrich (USA). Other chemicals were of analytical grade. The commercial contact lens cleaning solutions (3% H$_2$O$_2$) and antiseptic (30% H$_2$O$_2$) were purchased from local drug store. Double distilled deionized water was used throughout the experiments. All the experimental results were obtained at room temperature. Phosphate buffer solutions (PBS) (0.1 M, pH 7) for the

electro catalysis reactions were prepared from NaH$_2$PO$_4$–NaH$_2$PO$_4$ containing 1×10^{-3} M KI. Pure nitrogen was passed through all the experimental solutions.

2.2. Apparatus

Electrochemical measurements like cyclic voltammetry (CV), differential pulse voltammetry (DPV) were performed using CHI 410a and CHI 900 potentiostats (CH Instruments, Austin, TX). A conventional three-electrode system was used throughout the experiments. The BAS glassy carbon electrodes ($\varphi = 0.3$ cm in diameter) were in the form of disks sealed in a Teflon jacket having an exposed geometric surface area of 0.07 cm^2, respectively. The working electrode was a bare or nano TiO$_2$–Au–KI film modified GCE. The auxiliary electrode was a platinum wire and an Ag/AgCl electrode was used as a reference. All the potentials mentioned in this paper were referred to this reference electrode. The morphological characterizations of the film were studied by using SEM (Hitachi S-3000H) and AFM (Being Nano-Instruments CSPM-4000). Here for the convenience, indium tin oxide (ITO) thin film coated glass electrodes were used for SEM and AFM analysis.

2.3. Fabrication of nano TiO$_2$–Au–KI film modified GCE

Prior to electrode modification, the bare GCE was polished with the help of a BAS polishing kit with aqueous slurries of alumina powder (0.05 μm), rinsed and ultrasonicated in double distilled deionized water. After this process, the nano TiO$_2$ particles modified GCE was obtained by dipping the pretreated GCE in nano TiO$_2$ suspension (methanol solution) for 5 min. At this stage, a layer of nano TiO$_2$ was adsorbed on the GCE surface. Further the adsorbed nano TiO$_2$ modified GCE was washed carefully with double distilled water to remove the partially adsorbed nano TiO$_2$ particles. Next the gold nanoparticles were electrochemically deposited on the nano TiO$_2$ modified GCE from 0.5 M H$_2$SO$_4$ solution containing 1×10^{-3} M KAuCl$_4$·3H$_2$O by applying a repetitive potential scan between 1.1 and 0 V (vs. Ag/AgCl) at a scan rate of 100 mV s^{-1} for 30 cycles. Next, the electrochemical deposition of KI film on nano TiO$_2$–Au modified GCE was performed in pH 1.5 H$_2$SO$_4$ solution containing 1×10^{-3} M of KI by applying a repetitive potential scan between −0.75 and 1.2 V at 10 mV s^{-1} for 30 cycles. Finally, the nano TiO$_2$–Au–KI film modified electrode was fabricated. All the electrochemical reactions for nano TiO$_2$–Au–KI film were carried out in the buffer containing 1×10^{-3} M of KI for the electrochemical activation of the KI film.

3. Results and discussion

3.1. Characterization of nano TiO$_2$–Au–KI film modified GCE

In the past decade, the self-assembly method for nano TiO$_2$ film via alternative adsorption of oppositely charged substance materials has been developed [46–49]. Further on GCE, the adsorption of TiO$_2$ on hemoglobin/colloidal gold nanoparticles [50], manual coatings of nano TiO$_2$ have been reported [51]. Also, TiO$_2$ nanoparticles are readily adsorbed from aqueous acidic sols onto ceramic electrode surfaces such as tin-doped indium oxide (ITO)-coated glass electrodes [52–55]. In this study, the nano TiO$_2$ particles were adsorbed by dipping the pretreated GCE in methanol solution containing the nano TiO$_2$ suspensions. The time duration (5 min) is sufficient enough for the adsorption of nano TiO$_2$ on the GCE electrode surface. Next, Fig. 1 shows the cyclic voltammograms (CVs) of nano Au particles deposition on the nano TiO$_2$ modified GCE surface. Here the electrochemical depositions of Au nano particles occur with the growth of reduction and oxidation peaks at 0.6 and 1.1 V for 30 potential cycles. Further the significant growth of these
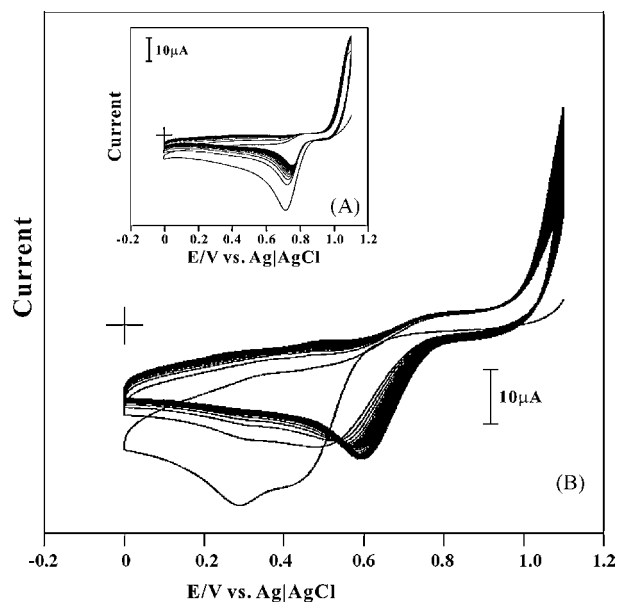
Fig. 1. Consecutive cyclic voltammograms of Au particles growth on nano TiO$_2$ modified GCE from 0.5 M H$_2$SO$_4$ containing 1×10^{-3} M KAuCl$_4 \cdot$3H$_2$O in the potential ranging from 0 to 1.1 V. The inset shows Au particles deposition on GCE in the same experimental condition (Scan rate = 100 mV s^{-1}).

peaks confirms the deposition of Au particles on the surface of nano TiO$_2$ particles modified GCE. To verify the presence of adsorbed nano TiO$_2$ on GCE, the cyclic voltammogram of Au particles deposition on nano TiO$_2$ modified GCE (Fig. 1) was compared with only Au particles deposition on GCE surface (inset of Fig. 1). For Au particles deposition process, the reduction peak of Au was appeared at 0.78 V. But, the reduction peak of Au at nano TiO$_2$ modified GCE was appeared at 0.6 V. Therefore, the shift in the reduction potential of Au authenticates the modification of the GCE with nano TiO$_2$ film, respectively. Hereafter the deposited Au particles will be denoted as nano Au particles. Finally, the electrochemical deposition of KI film was carried out on nano TiO$_2$–Au modified GCE. Thus, the nano TiO$_2$–Au–KI film modified GCE was fabricated.

Next the fabricated nano TiO$_2$–Au–KI film modified GCE was transferred to phosphate buffer solution (pH 7) containing 1×10^{-3} M of KI for the different scan rate studies (50–500 mV s^{-1}). Here the broad peak in reduction side attributed to the nano Au and KI film reduction and the oxidation peaks at 0.6 and 0.8 V attributed to the presence of KI film (Fig. 2). The electrochemical reduction
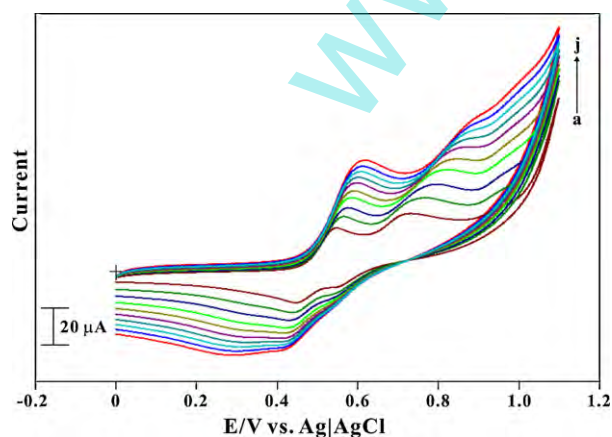
mechanism of nano Au is as follows [56,57];

$$AuCl_4^- + 3e^- \rightarrow Au^0 + 4Cl^- \tag{1}$$

Further for KI film, in anodic scan, it was oxidized first to triiodide (anodic peak 1) and then to iodine (anodic peak II). Further in the cathodic scan, the reduction of I$_3^-$ and I$_2$ occurs to I$^-$. Previous literatures report that this type of mechanism was verified by UV–vis spectroscopy in conjunction with cyclic voltammetry experiments at a thin gold mesh electrode [58,59]. The proposed electrochemical reaction mechanism of iodide is as follows;

$$3I^- \rightarrow I_3^- + 2e^- \tag{2}$$

$$2I_3^- \rightarrow 3I_2 + 2e^- \tag{3}$$

Furthermore, the presence of iodide layer is more electronegative and highly polarizable than nano Au and both the two redox couples were quasi reversible in this film. The peak to peak separations were slightly decreasing in higher scan rates. Furthermore, the plots of anodic and cathodic peak currents vs. scan rate (v) were linear in the range of 50–500 mV, suggests that it was surface-confined (figure not shown). At faster scan rates, the relationship becomes linear when the current values plotted vs. the square root of scan rate (v) (figure not shown), indicates the mass transport limited within the composite film. This is specifically true in a regime of high surface coverage, as it happens in the case of nano TiO$_2$–Au–KI film, and high sweep rates. Under these high sweep rates, the diffusion step dominates the procedure. Finally, above these results clearly illustrate the electrochemical activity of TiO$_2$–Au–KI film.

3.2. Influence of pH on nano TiO$_2$–Au–KI film modified GCE

In most cases, the solution pH is an important influence factor for the electrochemical reactions. Fig. 3 shows the influence of pH on nano TiO$_2$–Au–KI film modified GCE. As it can be seen that different cyclic voltammograms were observed for nano TiO$_2$–Au–KI film
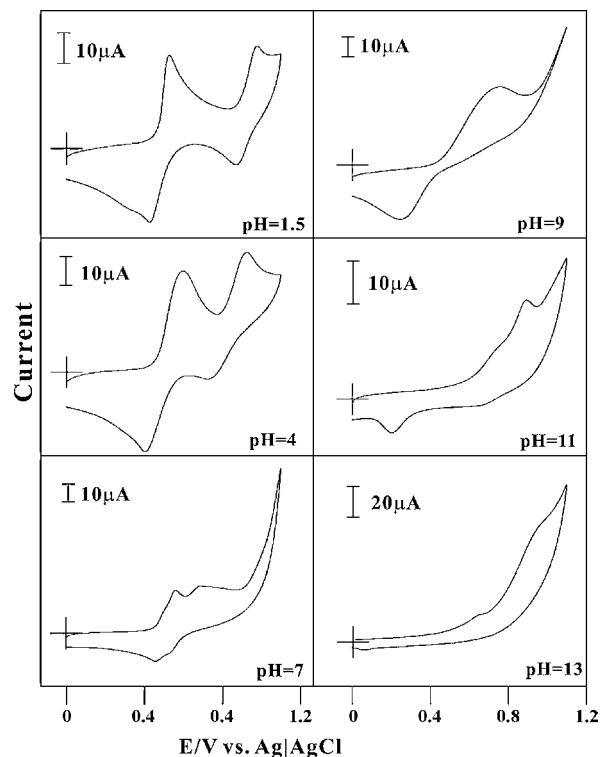

Fig. 2. Cyclic voltammograms nano TiO$_2$–Au–KI film modified GCE in pH 7.0 PBS solution containing 1×10^{-3} M KI for different scan rates (a–j); 50, 100, 150, 200, 250, 300, 350, 400, 450 and 500 mV s^{-1}.

Fig. 3. Cyclic voltammograms of nano TiO$_2$–Au–KI film modified GCE in various buffer solutions in presence of 1×10^{-3} M KI (Scan rate = 100 mV s^{-1}).

in various pH solutions. The nano TiO_2–Au–KI film exhibited two obvious redox couples at pH 1.5 which corresponds to the presence of KI in the film. In addition, the clear view of KI redox peaks shows that KI is more active in pH 1.5 solutions. Further In pH 4 buffer solutions, the film exhibits the two quasi reversible redox couples of KI film. Next in pH 7 solutions, the redox peaks of KI was not so active, exhibited as quasi reversible. At the same time, we could identify the sharp oxidation peaks of nano Au particles in this pH solution. Here the peak to peak separations of KI redox couples were very low comparing with pH 1.5 and 4 solutions. Next in pH 9 buffer solutions, it shows one quasi reversible redox peak at 0.3 and 0.8 V. Furthermore, in pH 11 it shows one reduction peak at 0.2 V and one oxidation peak at 8.8 V. In pH 13 buffer solutions, it shows only two oxidation peaks at 0.66 and 0.95 V. From these pH studies, it reveals that in pH 1.5, 4 and 7 buffer solutions nano TiO_2–Au–KI film is electrochemically active. For real sample analysis the physiological pH condition was required. Hence, pH 7 PBS solution was chosen for the electro catalytic reactions of nano TiO_2–Au–KI film.

3.3. SEM studies

Fig. 4A–D shows the typical SEM micrographs obtained for the adsorption of nano TiO_2, electrochemical depositions of flower shaped nano Au and nano TiO_2–Au–KI film fabrication on the ITO surface. Here the SEM Fig. 4A shows the 60° angle view of the adsorbed TiO_2 nano particles which were aggregated as a group of particles on the ITO surface. Further, Fig. 4A clearly authenticates the adsorption of nano TiO_2 particles as a group of aggregated particles on the ITO surface. Next, Fig. 4B shows the 90° angle view of the flower shaped gold nanoparticles electrodeposited on the ITO surface. This result validates the electrochemical deposition of gold nano particles formed in the flower shape and size varies from

230 nm to 1 μm. Especially, during the electrochemical deposition process, the individual Au nanoparticles will get together to form as a flower shape and exhibit the nano scale properties. In particular, the flower shaped gold nanoparticles will exhibit as active centers on the nano TiO_2 film surface. At the same time, Fig. 4C shows the 60° view angle of nano TiO_2–Au–KI film on ITO. Further from Fig. 4C and D, we could clearly identify the adsorption and electrochemical depositions of nano TiO_2 and Au particles, respectively. Here the KI film, which was electrodeposited as a thin layer cannot be identified from the nano TiO_2–Au–KI film surface. In addition, Fig. 4D shows the magnified view (90° angle) of Fig. 4C (20 μm). From these SEM results, the presence of nano TiO_2, and flower shaped gold nanoparticles were authenticated.

3.4. AFM studies

The AFM studies could furnish the comprehensive information about the surface morphology of nano TiO_2, flower shaped nano Au and KI film, respectively. Here the AFM parameters were evaluated for 20,000 nm × 20,000 nm surface area. The surface morphology of nano TiO_2–Au–KI film was examined by using the tapping mode. Fig. 5A illustrates the tapping mode image of nano TiO_2–Au–KI film. Fig. 5B–D shows the amplitude, phase and three dimensional view and Fig. 5E shows the cross-sectional view graph of the nano TiO_2–Au–KI film. From Fig. 5A, we could see the existence of nano TiO_2 and flower shaped nano Au particles in obvious manner. At the same time the electrochemical deposition of KI was fabricated as a thin layer on the nano TiO_2–Au film. Thus, the analysis of KI film is not obvious in the SEM and AFM analysis.

Furthermore, the morphological characteristic results of nano TiO_2–Au–KI film observed in AFM were consistent with their SEM results. Here the size of the nano TiO_2 and flower shaped Au
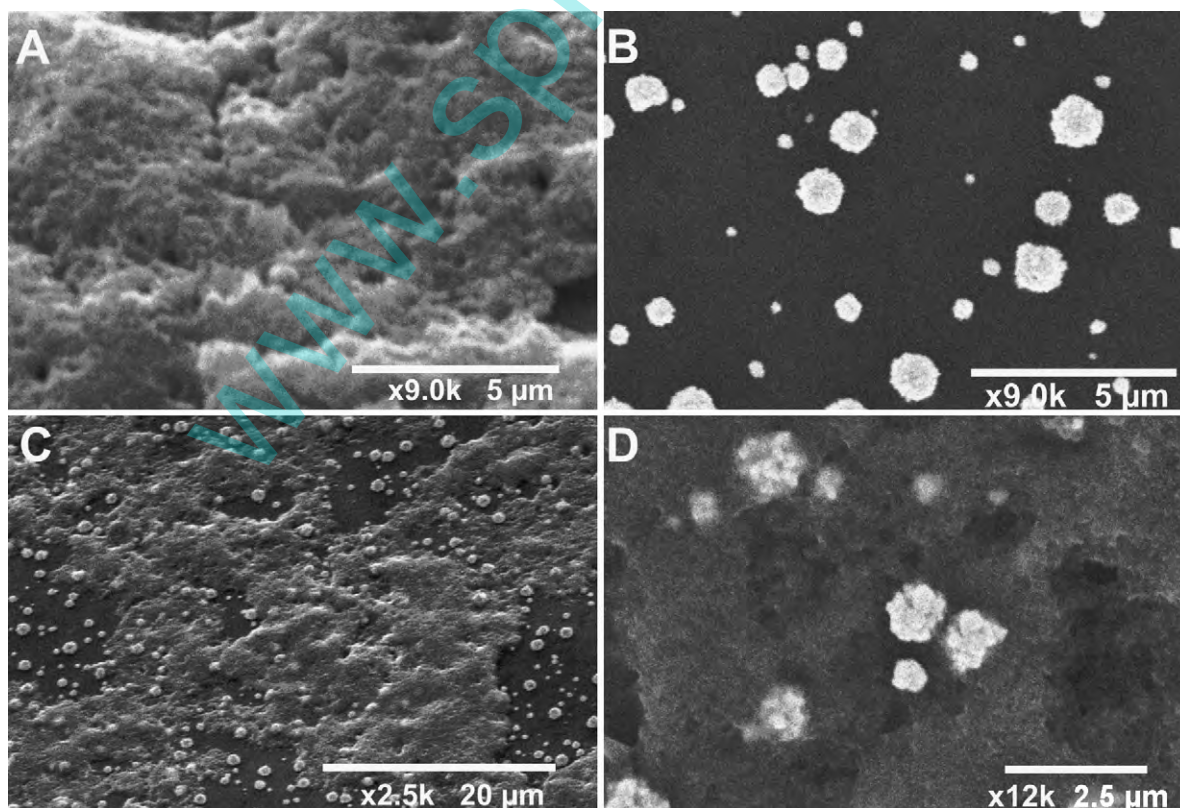

Fig. 4. (A) SEM image of the nano TiO_2 modified ITO (view angle 60°), (B) flower shaped nano Au on ITO (view angle 90°), (C) nano TiO_2–Au–KI film (view angle 60°) and (D) close view of the same film (view angle 90°).
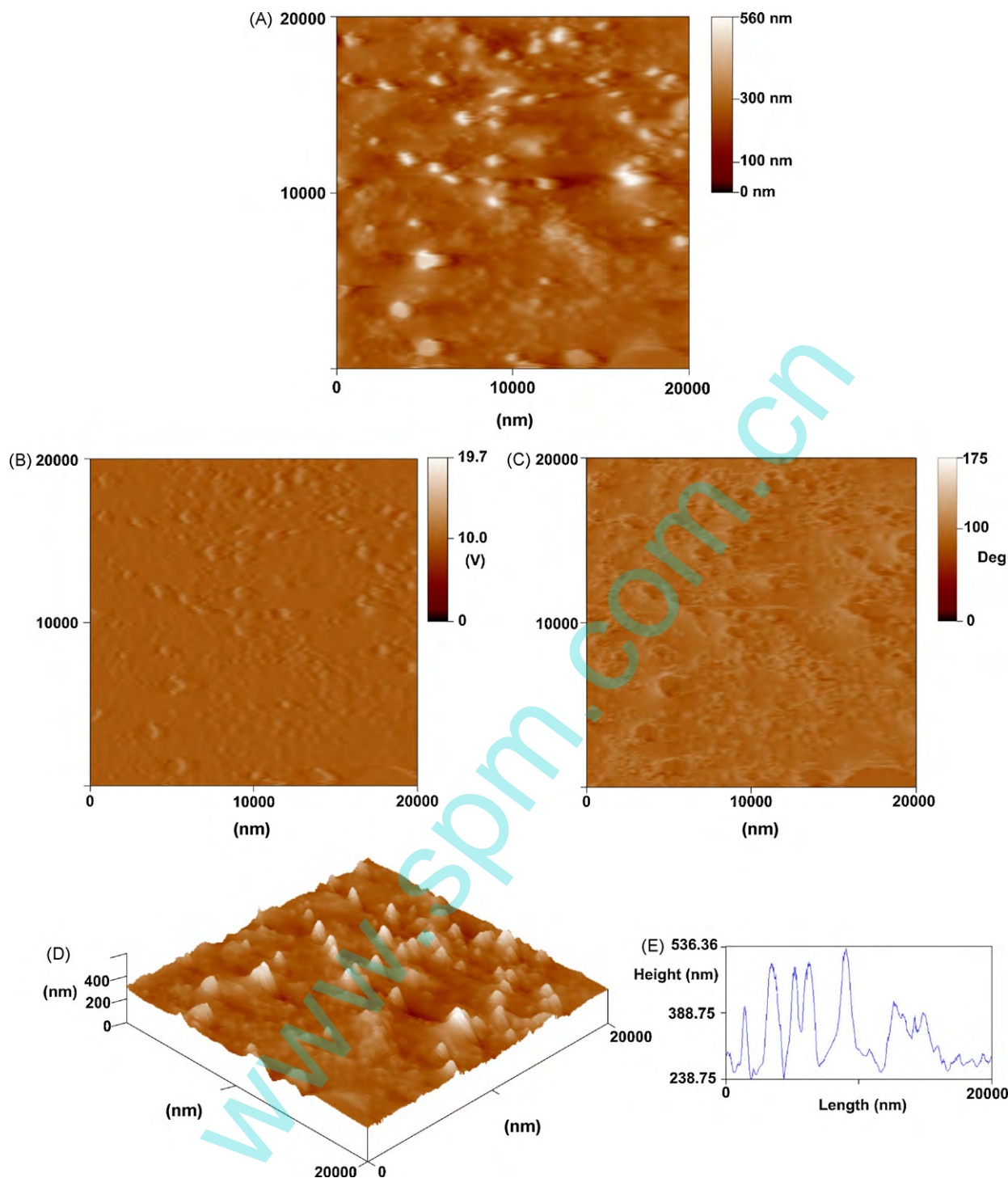
Fig. 5. Tapping mode AFM images of nano TiO_2–Au–KI film on ITO. (A) Topographic, (B) amplitude, (C) phase, (D) three dimensional view of TiO_2–Au–KI film on ITO and (E) cross-sectional graph of the nano TiO_2–Au–KI film.

nanoparticles observed were similar like in SEM. In addition, the other parameters such as the roughness average (sa) for nano TiO_2–Au film (20,000 nm × 20,000 nm) was found as 52 nm. Likewise, by using a combination of skewness and kurtosis values, it is possible to identify the film surfaces which have the relatively flat top and deep valleys. The skewness (Rsk) measures the symmetry of variation of the surface about its mean plane. The positive skewness value (1.02) of nano TiO_2–Au–KI film shows that the surface comprised of disproportionate number of peaks indicating the

uneven allocations of nano TiO_2 and flower shaped nano Au particles, respectively. Moreover, the kurtosis (Rku) is a measure of the unevenness or sharpness of the surface. A surface that is centrally distributed has a kurtosis value greater than 3. In this film, the kurtosis value was found as 3.53. The other functional parameters like the core roughness depth (Rk), surface bearing index (Rbi), and reduced valley depth (Rvk) were found as 109 nm, 0.941, 17.3 nm. Finally the above AFM results clearly illustrate the surface nature of the nano TiO_2–Au–KI film.
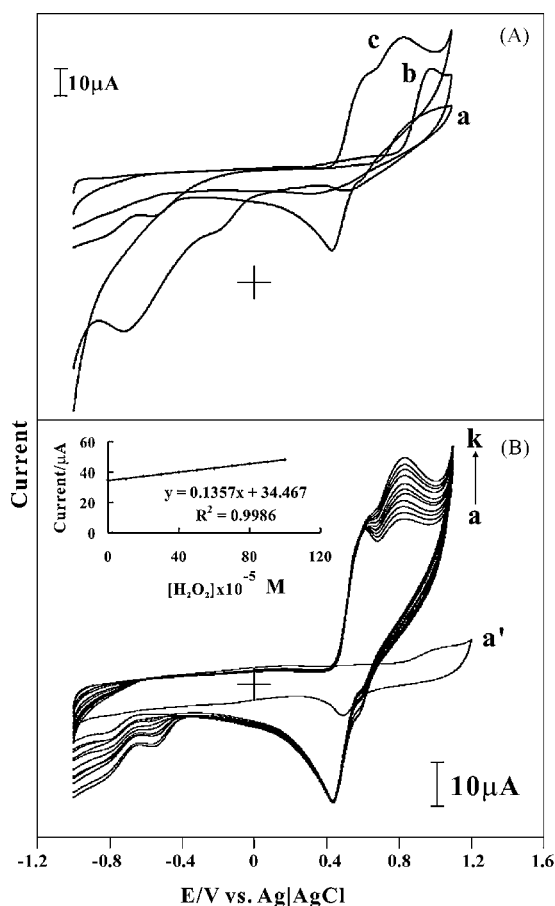
Fig. 6. (A) Cyclic voltammograms of (a) nano TiO$_2$–KI, (in presence of 1×10^{-3} M KI), (b) nano TiO$_2$–Au, (absence of 1×10^{-3} M KI) (c) nano TiO$_2$–Au–KI film modified GCE in pH = 7 PBS (in presence of 1×10^{-3} M KI) with the concentration of H$_2$O$_2$ 1×10^{-4} M. (B) Cyclic voltammograms nano TiO$_2$–Au–KI film modified GCE in presence of 1×10^{-3} M KI in a pH = 7 PBS solution with various concentration of H$_2$O$_2$ (a–k) 0, 1×10^{-5}, 2×10^{-5}, 3×10^{-5}, 4×10^{-5}, 5×10^{-5}, 6×10^{-5}, 7×10^{-5}, 8×10^{-5}, 9×10^{-5} and 1×10^{-4} M (a′) bare GCE and H$_2$O$_2$ 1×10^{-4} M (Scan rate = 100 mV s^{-1}).

3.5. Electrocatalytic oxidation of H$_2$O$_2$ on nano TiO$_2$–Au–KI film modified GCE

The electro catalytic oxidation of H$_2$O$_2$ on nano TiO$_2$–Au–KI film modified GCE was investigated by CV. According to the remarkable effect of pH on the peak potentials of nano TiO$_2$–Au–KI film and considering the physiological condition for real sample analysis, we have selected pH 7.0 PBS solutions for the electro catalytic oxidation of H$_2$O$_2$. In order to evaluate the electro catalytic activity of nano TiO$_2$–Au–KI film, it was compared with the other two films (nano TiO$_2$–KI, nano TiO$_2$–Au film) for H$_2$O$_2$ electrocatalytic oxidation process using CV (Fig. 6A). As shown, for H$_2$O$_2$ concentration (1×10^{-4} M), the anodic peak currents of nano TiO$_2$–Au–KI film was significantly higher than the anodic peak currents of nano TiO$_2$–KI and nano TiO$_2$–Au films, respectively. From these results, the need, purpose and the importance of nano TiO$_2$–Au–KI film was authenticated.

Further, Fig. 6B shows the cyclic voltammograms of nano TiO$_2$–Au–KI film modified GCE in the presence of H$_2$O$_2$ at pH 7.0 PBS buffer solution. Here the concentrations of H$_2$O$_2$ were in the linear range of 1×10^{-5} to 1×10^{-4} M, respectively. As shown for bare GCE (curve a′), no redox response of H$_2$O$_2$ (1×10^{-4} M) can be seen in the potential range from 0.8 to 1.2 V. However, at the nano TiO$_2$–Au–KI film modified GCE, the oxidation current of nano TiO$_2$–Au–KI film was greatly increased due to the electro catalytic oxidation of H$_2$O$_2$ (0.8 V), while the reduction peak of H$_2$O$_2$ appeared at -0.6 V. Fur-

ther the increasing peak currents of H$_2$O$_2$ oxidation confirms that the flower shaped nano Au particles have the higher catalytic ability together with nano TiO$_2$ and KI. From this result, it is evident that the presence of flower shaped nano Au will increase the electro catalytic activity of the film and act as active centers for this film [60]. Therefore, the nano TiO$_2$–Au–KI film are suitable mediators to transfer the electron between H$_2$O$_2$ and working electrode to facilitate the electrochemical regeneration of oxidized H$_2$O$_2$ in the reduction potentials. Further from the inset of Fig. 6B, the catalytic peak currents are proportional to the concentration of H$_2$O$_2$ in the range of 1×10^{-5} to 1×10^{-4} M. The linear regression equation for this concentration range is obtained as I_{pa} (μA) = 0.1357C (10^{-5} M) + 34.467 with the correlation coefficient of R^2 = 0.9986. Finally, these results prove the efficiency of nano TiO$_2$–Au–KI film for the significant detection of H$_2$O$_2$.

3.6. Differential pulse voltammetric studies

Generally in biomedical diagnostic applications, enzymes were employed to produce the redox active compound, such as H$_2$O$_2$. According to this point, there is a real challenge for the electrocatalysis of H$_2$O$_2$ in nanomolar concentrations. In this report, we examined the nano TiO$_2$–Au–KI film modified electrode for the detection of H$_2$O$_2$ in nanomolar concentrations. The differential pulse voltammetric technique could provide a better peak resolution and current sensitivity and most suitable for the electrocatalytic oxidation of H$_2$O$_2$. Since the DPV technique has been more sensitive than cyclic voltammetry, it has been employed to prove the film's performance for H$_2$O$_2$ electro oxidation reaction. Fig. 7 shows the DPVs of nano TiO$_2$–Au–KI film (pH 7 PBS) for the different concentrations of H$_2$O$_2$. Here the DPVs were recorded by sweeping the potentials in the range of 0–0.9 V at pulse amplitude of 50 mV, and a scan rate at 50 mV s^{-1}. Here the DPVs were recorded in the concentration range of 1×10^{-9} to 1×10^{-7} M H$_2$O$_2$, respectively. Fig. 7A, curve a–g shows the well-defined and stable anodic peak current curves for H$_2$O$_2$ oxidation. These anodic DPV curves confirm the H$_2$O$_2$ oxidation process on the TiO$_2$–Au–KI film modified GCE. Further the oxidation peak currents of H$_2$O$_2$ increases linearly with the increasing concentration of H$_2$O$_2$, respectively. The inset of Fig. 7 shows the current vs. concentration plot for the electrocatalytic oxidation of H$_2$O$_2$. In addition, the linear regression equation from the calibration plot for the oxidation of H$_2$O$_2$ is expressed as I_{pa} (μA) = 0.0576C (10^{-9} M) + 10.072 with a correla-
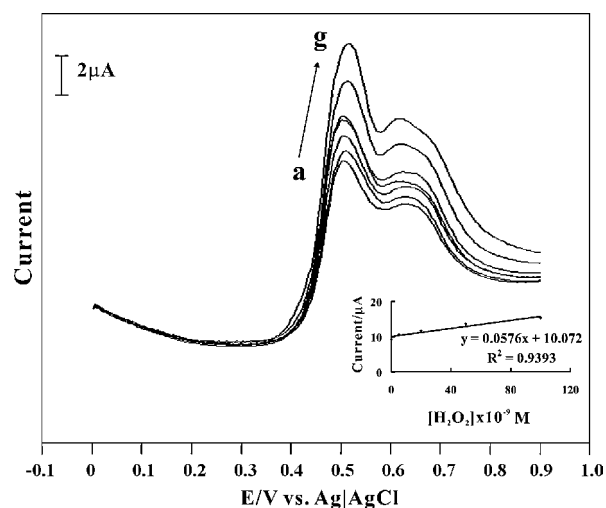

Fig. 7. Differential pulse voltammograms of nano TiO$_2$–Au–KI film modified GCE in pH = 7 PBS (containing 1×10^{-3} M KI) with various concentration of H$_2$O$_2$ (a–g) 0, 1×10^{-9}, 5×10^{-9}, 1×10^{-8}, 2×10^{-8}, 5×10^{-8} and 1×10^{-7} M.

Table 1
Comparison table of nano TiO_2–Au–KI film for H_2O_2 oxidation with previous literature report.

S. No.	Type of film modified electrode	H_2O_2 oxidation in linear range (M)	Electrolyte (phosphate buffer (pH))	Ref.
1.	Pt nanoparticle-CNT modified GCE	25×10^{-9} to 2×10^{-6}	7.2	[61]
2.	Nano TiO_2–Au–KI film modified GCE	1×10^{-9} to 1×10^{-7}	7.0	Proposed method

Table 2
H_2O_2 detection in real samples.

S. No.	Real samples	H_2O_2 detection (μM)		Recovery (%)
		Added	Found	
1.	Contact lens cleaner solution	2.6	2.7	103.8
		2.9	2.8	96.5
2.	Antiseptic solution	3.2	3.1	96.8
		3.5	3.6	102.8

tion coefficient of $R^2 = 0.9393$, respectively. From the above results, it shows that the nano TiO_2–Au–KI film modified GCE is effective for the electrocatalytic oxidation of H_2O_2 in nanomolar concentration range by using DPV techniques. Furthermore the comparison Table 1 could explain the performance the nano TiO_2–Au–KI film modified GCE with other modified electrodes.

3.7. Repeatability and stability of the proposed electrode

Ten replicate measurements ($n = 10$) were performed with the nano TiO_2–Au–KI film at the given H_2O_2 concentrations within the linear range displayed high reproducibility (2%). Further the stability of the film modified GC electrode was investigated by monitoring the higher concentration of H_2O_2 (1×10^{-4} M) solution for 4 h. In all these cases, the cyclic voltammograms and in particular the current signals appeared were stable (within 3%). Further these results show that the nano TiO_2–Au–KI film modified GCE possess good repeatability and stability.

3.8. Real sample analysis

To investigate the real applicability of nano TiO_2–Au–KI film for feasible usage, the concentration of H_2O_2 in two different types of real samples like contact lens cleaner solutions (3% H_2O_2), antiseptic solution (30% H_2O_2) were examined. Here the dilutions of real samples were employed with distilled water and pH 7.0 PBS to bring the H_2O_2 content with those shown in Table 2. The real samples analyses result for both two different types of samples (using standard addition method) are listed in Table 2. The agreeable recoveries were obtained by using the TiO_2–Au–KI film modified GCE confirms that the proposed film is suitable for the real sample analysis.

4. Conclusion

In conclusion, we have fabricated the nano TiO_2–Au–KI film sensor at GCE and ITO electrode surface by adsorption and electrochemical deposition methods. Further the fabricated nano TiO_2–Au–KI film, which was found as stable and electrochemically active in pH 1.5, 4 and 7.0 solutions. The surface morphology of nano TiO_2–Au–KI film was examined by SEM and AFM techniques. Further the nano TiO_2–Au–KI film showed good catalytic effect for H_2O_2 oxidation by using CV and DPV techniques, respectively. In particular, the present DPV investigations showed the higher electrocatalytic activity for the detection of H_2O_2 in nano molar concentrations. Furthermore, the proposed film showed sufficient results for the detection of H_2O_2 in the real sample analysis. Finally, this work illustrates a simple and novel approach for the hydrogen peroxide sensor fabrication based on nano TiO_2–Au–KI film.

References

[1] Y. Usui, K. Sato, M. Tanaka, Catalytic dihydroxylation of olefins with hydrogen peroxide: an organic-solvent-and metal-free system, Angew. Chem. 42 (2003) 5623–5625.
[2] E.A. Mazzio, K.F.A. Soliman, Glioma cell antioxidant capacity relative to reactive oxygen species produced by dopamine, J. Appl. Toxicol. 24 (2004) 99–106.
[3] M. Zayats, R. Baron, I. Popov, I. Willner, Biocatalytic growth of Au nanoparticles: from mechanistic aspects to biosensors design, Nano Lett. 5 (2005) 21–25.
[4] P.A. Tanner, A.Y.S. Wong, Spectrophotometric determination of hydrogen peroxide in rainwater, Anal. Chim. Acta 370 (1998) 279–287.
[5] N.V. Klassen, D. Marchington, H.C.E. McGovan, H_2O_2 determination by the I_3^- method and by $KMnO_4$ titration, Anal. Chem. 66 (1994) 2921–2925.
[6] O.S. Wolfbeis, A. Durkop, M. Wu, Z. Lin, A europium-ion-based luminescent sensing probe for hydrogen peroxide, Angew. Chem. Int. Ed. 41 (2002) 4495–4498.
[7] X. Shu, Y. Chen, H. Yuan, S. Gao, D. Xiao, H_2O_2 sensor based on the room-temperature phosphorescence of nano TiO_2/SiO_2 composite, Anal. Chem. 79 (2007) 3695–3702.
[8] U. Pinkernell, S. Effkemann, U. Karst, Simultaneous HPLC determination of peroxyacetic acid and hydrogen peroxide, Anal. Chem. 69 (1997) 3623–3627.
[9] S.A. Kumar, S.-M. Chen, Myoglobin/arylhydroxylamine film modified electrode: direct electrochemistry and electrochemical catalysis, Talanta 72 (2007) 831–838.
[10] G. Decher, Fuzzy nanoassemblies: toward layered polymeric multicomposites, Science 277 (1997) 1232–1237.
[11] C. Li, C. Wang, S. Hu, Development of a parathion sensor based on molecularly imprinted nano-TiO_2 self-assembled film electrode, Sens. Actuators, B, Chem. 117 (2006) 166–171.
[12] A. Salimi, E. Sharifi, A. Noorbakhask, S. Soltanian, Direct voltammetry and electrocatalytic properties of hemoglobin immobilized on a glassy carbon electrode modified with nickel oxide nanoparticles, Electrochem. Commun. 8 (2006) 1499–1508.
[13] G. Zhao, J.J. Xu, H.Y. Chen, Fabrication, characterization of Fe_3O_4 multilayer film and its application in promoting direct electron transfer of hemoglobin, Electrochem. Commun. 8 (2006) 148–154.
[14] G. Zhao, J.J. Feng, J.J. Xu, H.Y. Chen, Direct electrochemistry and electrocatalysis of heme proteins immobilized on self-assembled ZrO_2 film, Electrochem. Commun. 7 (2005) 724–729.
[15] J.J. Feng, J.J. Xu, H.Y. Chen, Direct electron transfer and electrocatalysis of hemoglobin adsorbed onto electrodeposited mesoporous tungsten oxide, Electrochem. Commun. 8 (2005) 77–82.
[16] Y. Lvov, B. Munge, O. Giraldo, I. Ichinose, S. Suib, J.F. Rusling, Films of manganese oxide nanoparticles with polycations or myoglobin from alternate-layer adsorption, Langmuir 16 (2000) 8850–8857.
[17] A. Salimi, R. Hallaj, S. Soltanian, H. Mamkhezria, Nanomolar detection of hydrogen peroxide on glassy carbon electrode modified with electrodeposited cobalt oxide nanoparticles, Anal. Chim. Acta 594 (2007) 24–31.
[18] P.A. Van Hal, M.M. Winkm, J.M. Kroon, W.J.H. Verhees, L.H. Slooff, W.J.H. van Gennip, P. Johkeijm, R.A.J. Janssen, Photo induced electron transfer and photovoltaic response of a MDMO-PPV:TiO_2 bulk-hetero junction, Adv. Mater. 15 (2003) 118–121.
[19] U. Bach, D. Lupo, P. Comte, J.E. Moser, F. Weissörtel, J. Salbeck, H. Spreitzer, M. Grätzel, Solid-state dye-sensitized mesoporous TiO_2 solar cells with high photon-to-electron conversion efficiencies, Nature 395 (1998) 583–585.
[20] L. Kavan, M. Grätzel, S.E. Gilbert, C. Klemenz, H.J. Scheel, Electrochemical and photoelectrochemical investigation of single-crystal anatase, J. Am. Chem. Soc. 118 (1996) 6716–6723.
[21] J.M. Macak, P.J. Barczuk, H. Tsuchiya, M.Z. Nowakowska, A. Ghicov, M. Chojak, S. Bauer, S. Virtanen, P.J. Kulesza, P. Schmuki, Self-organized nanotubular TiO_2 matrix as support for dispersed Pt/Ru nanoparticles: enhancement of the electrocatalytic oxidation of methanol, Electrochem. Commun. 7 (2005) 1417–1422.
[22] A. Ghicov, J.M. Macak, H. Tsuchiya, J. Kunze, V. Heaublein, L. Frey, P. Schmuki, Ion implantation and annealing for an efficient N-doping of TiO_2 nanotubes, Nanoletters 6 (2006) 1080–1082.
[23] H. Tsuchiya, J.M. Macak, L. Muller, J. Kunze, F. Muller, S.P. Greil, S. Virtanen, P. Schmuki, Hydroxyapatite growth on anodic TiO_2 nanotubes, J. Biomed. Mater. Res. 77 (2006) 534–541.

[24] J.H. Kim, S.H. Kim, S. Shiratori, Fabrication of nanoporous and hetero structure thin film via a layer-by-layer self assembly method for a gas sensor, Sens. Actuators, B, Chem. 102 (2004) 241–247.

[25] X. Zhang, G. Yan, H. Ding, Y. Shan, Fabrication and photovoltaic properties of self-assembled sulfonated polyaniline/TiO₂ nano composite ultrathin films, Mater. Chem. Phys. 102 (2007) 249–254.

[26] J. Wang, L. Fang, D. Lopez, H. Tobias, Highly selective and sensitive amperometric biosensing of glucose at ruthenium-dispersed carbon paste enzyme electrodes, Anal. Lett. 26 (1993) 1819–1830.

[27] C.M. Welch, C.E. Banks, A.O. Simm, R.G. Compton, Silver nanoparticle assemblies supported on glassy-carbon electrodes for the electro-analytical detection of hydrogen peroxide, Anal. Bioanal. Chem. 382 (2005) 12–21.

[28] J. Li, Q. Yu, T. Peng, Electrocatalytic oxidation of hydrogen peroxide and cysteine at a glassy carbon electrode modified with platinum nanoparticle-deposited carbon nanotubes, Anal. Sci. 21 (2005) 377–381.

[29] W. Yang, Y. Li, Y. Bai, C. Sun, Hydrogen peroxide biosensor based on myoglobin/colloidal gold nanoparticles immobilized on glassy carbon electrode by a Nafion film, Sens. Actuators, B, Chem. 115 (2006) 42–48.

[30] J. Wang, L. Angnes, Miniaturized glucose sensors based on electrochemical co deposition of rhodium and glucose oxidase onto carbon-fiber electrodes, Anal. Chem. 64 (1992) 456–459.

[31] P.C. Biswas, Y. Nodasaka, M. Enyo, M. Haruta, Electro-oxidation of CO and methanol on graphite-based platinum electrodes combined with oxide-supported ultrafine gold particles, J. Electroanal. Chem. 381 (1995) 167–177.

[32] M.-C. Daniel, D. Astruc, Gold nanoparticles: assembly, supramolecular chemistry, quantum-size-related properties, and applications toward biology, catalysis, and nanotechnology, Chem. Rev. 104 (2004) 293–346.

[33] C.-H. Kuo, M.H. Huang, Synthesis of branched gold nanocrystals by a seeding growth approach, Langmuir 21 (2005) 2012–2016.

[34] M. Zhou, S. Chen, S. Zhao, Synthesis of icosahedral gold nanocrystals: a thermal process strategy, J. Phys. Chem. B 110 (2006) 4510–4513.

[35] B.K. Jena, C.R. Raj, Synthesis of flower-like gold nanoparticles and their electrocatalytic activity towards the oxidation of methanol and the reduction of oxygen, Langmuir 23 (2007) 4064–4070.

[36] V. Iliev, D. Tomova, L. Bilyarska, G. Tyuliev, Influence of the size of gold nanoparticles deposited on TiO₂ upon the photocatalytic destruction of oxalic acid, J. Mol. Catal. A: Chem. 263 (2007) 32–38.

[37] B. Zhu, Q. Guo, X. Huang, S. Wang, S. Zhang, S. Wu, W. Huang, Characterization and catalytic performance of TiO₂ nanotubes-supported gold and copper particles, J. Mol. Catal. A: Chem. 249 (2006) 211–217.

[38] A. Mirescu, H. Berndt, A. Martin, Ulf Prüße, Long-term stability of a 0.45% Au/TiO₂ catalyst in the selective oxidation of glucose at optimised reaction conditions, Appl. Catal., A: Gen. 317 (2007) 204–209.

[39] E.V. Milsoma, J. Novaka, M. Oyama, F. Markena, Electrocatalytic oxidation of nitric oxide at TiO₂–Au nanocomposite film electrodes, Electrochem. Commun. 9 (2007) 436–442.

[40] Y.-T. Shi, R. Yuan, Y.-Q. Chai, X.-L. He, Development of an amperometric immunosensor based on TiO₂ nanoparticles and gold nanoparticles, Electrochim. Acta 52 (2007) 3518–3524.

[41] D. Jašin, A.A. Rabi, S. Mentus, D. Jovanovic, Oxygen reduction reaction on spontaneously and potentiodynamically formed Au/TiO₂ composite surfaces, Electrochim. Acta 52 (2007) 4581–4588.

[42] M.R. Miah, T. Ohsaka, Enhanced electrochemical oxidation of H₂O₂ at iodine-modified gold electrode in alkaline media, J. Electrochem. Soc. 153 (12) (2006) E195–E200.

[43] A.T. Hubbard, Electrochemistry at well-characterized surfaces, Chem. Rev. (Washington, DC) 88 (1998) 633–656.

[44] S. Sugita, T. Abe, K. Itaya, Electrochemical scanning tunneling microscopy of silver adlayers on iodine-coated gold(111) in perchloric acid solution, J. Phys. Chem. 97 (1993) 8780–8785.

[45] M.R. Miah, T. Ohsaka, Cathodic detection of H₂O₂ using iodide-modified gold electrode in alkaline media, Anal. Chem. 78 (2006) 1200–1205.

[46] G. Decher, J.D. Hong, J. Schmit, Buildup of ultrathin multilayer films by a self-assembly process: III. Consecutively alternating adsorption of anionic and cationic polyelectrolytes on charged surfaces, Thin Solid Films 210–211 (1992) 831–835.

[47] Y. Tsuge, K. Inokuchi, K. Onozuka, O. Shingo, S. Sugi, M. Yoshikawa, S. Shiratori, Fabrication of porous TiO₂ films using a spongy replica prepared by layer-by-layer self-assembly method: application to dye-sensitized solar cells, Thin Solid Films 499 (2006) 396–401.

[48] J. Li, H.-C. Zeng, Preparation of monodisperse Au/TiO₂ nanocatalysts via self-assembly, Chem. Mater. 18 (2006) 4270–4277.

[49] C.-H. Huang, C.-H. Huang, T.-P. Nguyen, C.-S. Hsu, Self-assembly monolayer of anatase titanium oxide from solution process on indium tin oxide glass substrate for polymer photovoltaic cells, Thin Solid Films 515 (2007) 6493–6496.

[50] W.W. Yang, Y. Bai, Y. Li, C. Sun, Amperometric nitrite sensor based on hemoglobin/colloidal gold nanoparticles immobilized on a glassy carbon electrode by a titania sol–gel film, Anal. Bioanal. Chem. 382 (2005) 44–50.

[51] S. Yuan, S.H. Hu, Characterization and electrochemical studies of Nafion/nano-TiO₂ film modified electrodes, Electrochim. Acta 49 (2004) 4287–4293.

[52] E. Stathatos, P. Lianos, Photophysical properties of an amphiphilic cationic hemicyanine dye in solution and adsorbed on a TiO₂ mesoporous film, Langmuir 13 (1997) 259–263.

[53] K.J. McKenzie, F. Marken, Accumulation and reactivity of the redox protein Cytochrome c in mesoporous films of TiO₂ phytate, Langmuir 19 (2003) 4327–4331.

[54] C.A. Paddon, F. Marken, Hemoglobin adsorption into TiO₂ phytate multi-layer films: particle size and conductivity effects, Electrochem. Commun. 6 (2004) 1249–1253.

[55] E.V. Milsom, H.A. Dash, T.A. Jenkins, M. Opallo, F. Marken, The effects of conductivity and electrochemical doping on the reduction, of methemoglobin immobilized in nanoparticulate TiO₂ films, Bioelectrochemistry 70 (2007) 221–227.

[56] A.I. Gopalan, K.-P. Lee, K.M. Manesh, P. Santhosh, J.H. Kim, Gold nanoparticles dispersed into poly(aminothiophenol) as a novel electrocatalyst—fabrication of modified electrode and evaluation of electrocatalytic activities for dioxygen reduction, J. Mol. Catal. A: Chem. 256 (2006) 335–345.

[57] K.B. Holt, G. Sabin, R.G. Compton, J.S. Foord, F. Marken, Reduction of tetrachloroaurate (III) at boron-doped diamond electrodes: gold deposition versus gold colloid formation, Electroanalysis 14 (2002) 797–803.

[58] K.J. Hanson, M.J. Matlosz, C.W. Tobias, J. Newman, Electrochemistry of iodide in propylene carbonate, J. Electrochem. Soc. 134 (1987) 2204–2210.

[59] O. Chailapakul, M. Amatatongchai, P. Wilairat, K. Grudpan, D. Nacapricha, Flow-injection determination of iodide ion in nuclear emergency tablets, using boron-doped diamond thin film electrode, Talanta 64 (2004) 1253–1258.

[60] Y. Li, G. Shi, Electrochemical growth of two-dimensional gold nanostructures on a thin polypyrrole film modified ITO electrode, J. Phys. Chem. B 109 (2005) 23787–23793.

[61] S. Hrapovic, Y. Liu, K.B. Male, J.H. Luong, Electrochemical biosensing platforms using platinum nanoparticles and carbon nanotubes, Anal. Chem. 76 (2004) 1083–1088.

Biographies

Soundappan Thiagarajan completed his B.Sc. degree at Thiruvalluvar Government Arts and Science College, India and his M.Sc. degree at Department of Chemistry, Sri Ramakrishna Mission Vidyalaya College of Arts and Science, India. Since 2005 he is a Ph.D. candidate under the supervision of Prof. Shen-Ming Chen in Department of Chemical Engineering and Biotechnology, National Taipei University of Technology, Taiwan. His research interests include characterization of nano metals, nano-bi-metallic sensor materials, thick and thin-film devices, oxide electronics, semiconductor and ferroelectric films for biosensor applications. His special interest is in Scanning Electrochemical Microscopic techniques (SECM) for electrochemical imaging.

Buo-Wei Su obtained his M.S. degree (2007) under the supervision of Prof. Shen-Ming Chen at Department of Chemical Engineering and Biotechnology, National Taipei University of Technology, Taiwan. His research interest in M.S. study is mainly focused in nano metals, nano-bi-metallic materials and self-assembled monolayers for electrochemical and biosensor applications.

Shen-Ming Chen is a Professor in the Department of Chemical Engineering and Biotechnology, National Taipei University of Technology, Taiwan. Prof. Shen-Ming Chen obtained his Ph.D. in the Department of Chemistry, National Taiwan University, Taiwan and also persuaded as a visiting post-doctorial fellow in Institute of Inorganic Chemistry, University of Erlangen-Nuremberg, Germany. His research interests are based on the designing of various electrochemical and analytical devices such as biosensors and chemical sensors, sensors based on nanomaterials and the development of different kinds of electroanalytical methods and its application in biochemical and new analytical systems. Not only limited to this, he also interested in fuel cells and photovoltaic cells development.